Experimental investigation of heat transfer characteristic in supersonic flow field on a sharp fin shape

J.W. Song[1], J.J. Yi[1], M.S. Yu[2], H.H. Cho[1], K.Y. Hwnag[3], and J.C. Bae[3]

[1] *Department of Mechanical Engineering, Yonsei University, 120-749, Republic of Korea*
[2] *Department of Mechanical Engineering, Yonsei University, 120-749, Republic of Korea, presently National Science Museum Planning Office, Ministry of Science and Technology, 427-060, Republic of Korea*
[3] *Agency for Defense Development, P.O. Box 35, Yuseong, Daejeon*

1 Introduction

The development of a supersonic speed flight, one problem of practical importance is the inviscid/viscous interaction between shock wave and turbulent boundary layer. High local surface heat transfer could cause the burn-out of important units protruded into a supersonic flow field. Also, the large spatial difference of heating rates could bring a large thermal stress on a vehicle surface. For last decades, many researchers have tried to understand the flow structure and heat transfer phenomena near the protruding body in a supersonic flow. Aso[1] has measured pressure and heat flux distribution in the separated flow region by sharp fin and Stanton number is calculated from the measured heat flux. He showed the increase in pressure distribution and heat transfer in a separated and a reattachment flow region. However, this test needs a long test time for measuring two-dimensional distribution with 10 array sensors. Alvi[2] showed the sharp fin generating lambda-shock structure by using PLS (Planar Laser Scattering) imaging technique. But the investigation focused only on a shock visualization. Lu[3] proposed the correlation between a Mach number and an angle made by inviscid shock wave trace. But Lu's experiment also did not contain the pressure and heat transfer distribution data either. Knight[4] has conducted the numerical simulation and the experiment for the backward of a sharp fin in supersonic turbulent flow. Rodi[5] has studied the comparison of pressure distributions between a sharp and a blunt fin. Even in this test, he failed to include the heat transfer distribution to the results. In this study, heat transfer near a sharp fin was investigated. The fin rotating angle is considered as a parameter. We took the surface temperature images using an infra-red camera for the turbulent flow separated regions near sharp fins. To satisfy the constant heat flux condition on a surface, we made a thin foil heater which can be installed to the bottom surface near the fin. For the understanding of flow characteristics around a fin, the oil-lampblack method was also conducted.

2 Experimental Program

2.1 Supersonic blow-down tunnel

Figure 1 is the schematic diagram of the blow-down tunnel used in this study. Before the tunnel, there are the high pressure flow generating equipments consisting of air compressor, buffer, filters and storage tanks. The compressor can compress the air up to

20MPa and the pressurized air is stored to air tanks whose storage capacity is $1.8m^3$, respectively. Compressed air is going through the buffer tank and cooled down. When experiment starts, the compressed air is supplied from tanks to the stagnation chamber lowering its pressure level 150 to 6 down by a pressure regulator. In the inlet part of stagnation chamber, the cone-type separator and the 5 stages screen are installed to increase the flow uniformity and the lower turbulence level in a stagnation chamber. Settled flow in a stagnation chamber is accelerated through a supersonic nozzle whose designed Mach number of nozzle is three. The accelerated flow enters into the test chamber, where the pressure transducer and the windows for shock visualization are prepared. After the test chamber, the diffuser and the silencer are positioned for the pressure recovery and the noise reduction, respectively.

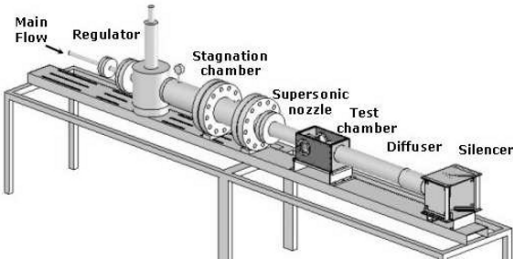

Fig. 1. Schematic diagram of Supersonic blow-down tunnel

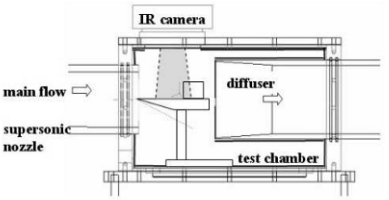

Fig. 2. Schematic diagram of Test Chamber

2.2 Test model and other supplement equipments

Figure 2 is the schematic diagram of a test chamber. Test chamber is located between a forward nozzle and a backward diffuser. And test model, which is installed inside of test chamber, is generated shock wave. When the experiment is started supersonic air is passes around a fin and motivating shock wave. This shock wave could interact with a boundary layer resulting in the change of surface temperature distribution and these variations of temperature were measured by an infra-red camera. During the test, a test chamber should be maintained in a nearly vacuum state. Therefore, the test chamber should be tightly sealed up after installing the test model and an infra-red camera. Sharp fin was used as a protruded body and the fin-installed test model is illustrating well Fig. 3. Fin was made of Aluminum. In a sharp fin case, the considered wedge angle were 12.5 °,15 °,17.5 °, and 20 °. All fins were unswept type. To produce a constant heat flux condition on a considered surface around the fin, the thin foil heater is designed and manufactured. The total thickness of a heater is 0.2mm. The electric resistance is 200Ω for a sharp fin. Heater were adhered to the teflon block by RTV. Below the thin foil heater, the teflon block and the mineral wool are positioned as thermal insulators with thickness and respectively as shown in Fig. 3. The infer-red camera has a 0.03K resolution and its frequency is almost 1Hz. And also camera has spatial resolution of 300×200 pixel. On the most of test model and test chamber, the flat black lacquer sprayed and its emissivity is found to be about 0.89 from the calibration test and is considered when the result of

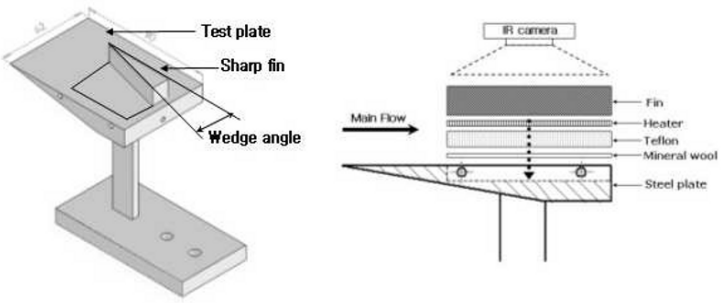

Fig. 3. Illustration of Sharp fin and Test plate

infra-red image is processed to calculate the surface distribution on a surface. To the foil heater, the direct current is supplied by the power whose maximum voltage and current are 200V and 20A, respectively. And the current value is monitored during the test by checking the voltage drop across the shunt positioned in the middle of an electric circuit. The most of voltage signals from sensors such as pressure transducer and thermocouples are received by the voltmeter and processed in a computer.

2.3 Experimental condition and test procedure

The upstream Mach number is about 3 and the unit Reynolds number in an free stream is about $5 \times 10^7/m$, respectively. Figure 4 shows the pressure and the temperature in the stagnation chamber and the pressure in a test chamber during the test. During the test, stagnation and test chamber pressure are almost maintained to be 6atm and 0.16atm, respectively. The stagnation chamber temperature also reaches to the steady state condition in nearly ten seconds although slight decrease is observed due to the gas expansion in air tanks and the Joule-Thompson effect at the valve and the pressure regulator. In this condition, Mach number is about three which is calculated by equation 1 as follows.

$$\frac{P_0}{P} = \left[1 + \frac{(k-1)}{2} M^2\right]^{\frac{k}{k-1}} \tag{1}$$

The experiments are conducted under the constant heat flux condition. Heat flux was calculated by equation 2.

$$\dot{q} = \dot{q}_g - \dot{q}_l \tag{2}$$

$\dot{q_g} = I^2 R$: generating heat flux on heater
$\dot{q_l}$: heat loss in the backward of the test plate
I : measured electrical current , R : electrical resistance of a thin foil heater

By the analysis of 1-dimensional transient conduction problem, heat loss is estimated to be about 8% when heat flux is $23,000 W/m^2$.
Heat transfer coefficient is calculated by following equation 3.

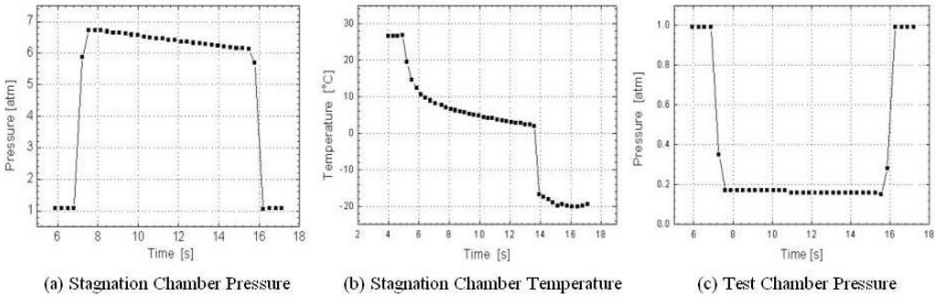

(a) Stagnation Chamber Pressure (b) Stagnation Chamber Temperature (c) Test Chamber Pressure

Fig. 4. Graph of chamber pressure and temperature

$$h = \frac{\dot{q}}{T_w - T_{aw}} \left[1 - (\frac{\xi}{x})^{0.9} \right]^{-\frac{1}{9}} \tag{3}$$

T_w : measured surface temperature
$T_{aw} = T_0 \frac{1+r\frac{k-1}{2}Ma^2}{1+\frac{k-1}{2}Ma^2}$: adiabatic wall temperature
r, k and Ma are the freestream recovery factor, specific heat ratio and Mach number.

3 Discussion of Results

3.1 Oil and lampblack method

We used oil and lampblack method in order to see the surface flow streak line which can be varied by the flow field change due to a protruded fin. We spread on the smooth surface of the test plate the mixture of carbon powder and silicon oil that is viscous enough not to be flown off in the flow. Figure 5 is the picture of streak line of sharp fin with a wedge angle of 20 degree. In Fig. 5, both of 1st and 2nd separation lines can be observed. These separation lines are also observed in case of wedge angles of 12.5 ° and 17.5 ° in Fig. 6.

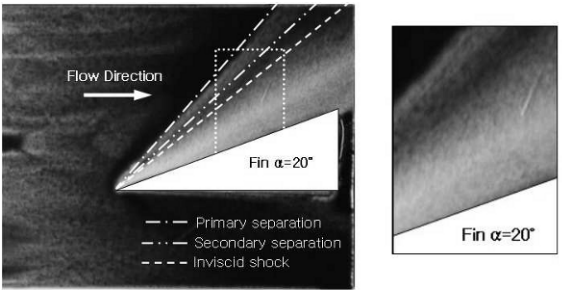

Fig. 5. Flow visualization by oil and lampblack

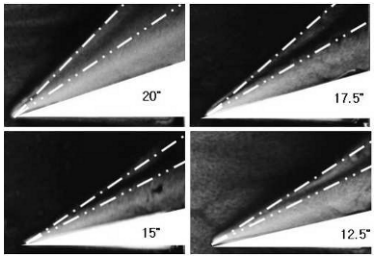

Fig. 6. Flow visualization by oil and lampblack on different wedge angle sharp fin

For the relation between fin wedge angle and 1st separation line angle , linear correlation equation is obtained and plotted in Fig. 7 together with an experimental result. First flow separation line is known to appear slightly ahead of the inviscid shock wave line. This flow separation in an upstream of inviscid shock wave is induced due to the upstream propagation of an increased pressure by the interaction between an inviscid shock wave and a boundary layer. Secondary separation line tends to be obscure with decreasing fin wedge angle. Especially, in a case of fin wedge angle less than 12.5 °, the secondary separation line cannot be observed.

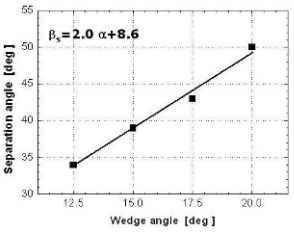

Fig. 7. Plot of 1st separation line angles to fin wedge angle

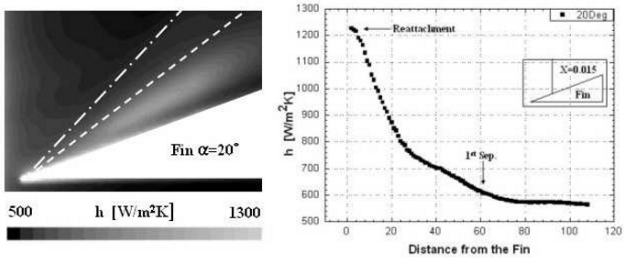

Fig. 8. Convective heat transfer coefficient distribution of sharp fin

3.2 Convective heat transfer coefficient

Convective heat transfer coefficient was calculated by surface temperature distribution with an infra-red thermography. Figure 8 shows an obtained distribution of convective heat transfer coefficient for the case of fin wedge angle 20 °. 1st separation line and inviscid shock line were also illustrated in Fig. 8 for reference. Heat transfer coefficient starts to increase gradually in a downstream from the point of flow separation. It has the highest value of $1200 W/m^2K$ at the region expected as a reattachment region. It is 2.5 times as high in that of the region where there is no interference between a boundary layer and a shock wave. The reason for this is as follows: Separated boundary layer flow impinges the flat surface in the region between fin and inviscid shock with a high turbulence level resulting in a high heat transfer. Heat transfer coefficient and pressure distribution are shown in Fig. 9. In this figure, it can be found that the second flow separation does not affect the heat transfer phenomena while the surface pressure changes largely. Figure 10 shows the more wedge angle increases, the more peak heat transfer coefficient value increases. Also, as the angle of the inviscid shock wave increases, the area becomes resulting in a wide heat transfer promoted area as shown in Fig. 10.

4 Conclusion

In this study, aerodynamic heating phenomena caused by interaction of shock wave with the turbulent boundary layer was investigated. An experimental study was performed for convective heat transfer around fin in supersonic flow field. During the experiment,

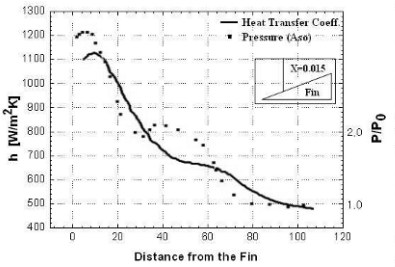

Fig. 9. Comparison with pressure and heat transfer coefficient distribution on sharp fin

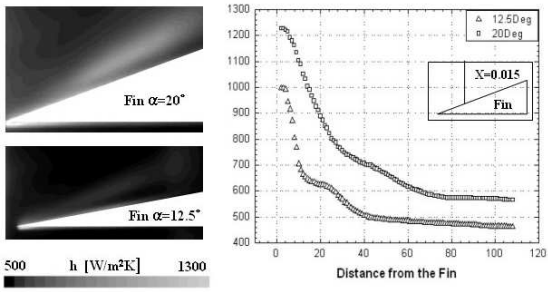

Fig. 10. Convective heat transfer coefficient distribution for different wedge angle

the wedge angle is considered as a parameter. Convective heat transfer coefficient of sharp fin increase gradually after 1st separation line. We found that the peak value of heat transfer coefficient appears at the location where the flow reattachment is expected. Distributions of pressure and heat transfer coefficient are similar in most area but 2nd separation did not affect on distribution of heat transfer coefficient unlike distribution of pressure. The distribution of heat transfer coefficient for sharp fin at the expected region of reattachment is 2.5 times higher than that of none interference region. The value of heat transfer coefficient increases with wedge angle. As wedge angle increasing, high heat transfer coefficient maintained region is also increasing.

Acknowledgement. This work was supported by Defense Acquisition Program Administration and Agency for Defense Development under the contract UD060016AD.

References

1. Shigeru Aso, Masanori Hayashi and Anzhong Tan : The Structure of Aerodynamic Heating in Three-Dimensional Shock Wave/Turbulent Boundary Layer Interactions Induce by Sharp Fin and Blunt Fins. AIAA, 89-1854
2. F. S. Alvi and G. S. Settles : Physical Model of the Swept Shock Wave/Boundary-Layer Interaction Flow Field. AIAA Jouna , Vol. 30, No. 9, September 1992
3. F. K. Lu, G. S. Settles and C. C. Horstman : Mach Number Effects on Conical Surface Features of Swept Shock-Wave/Boundary-Layer Interactions, AIAA Jounal, Vol. 28, No. 1, January 1990
4. Doyle D. Knight, T.J. Garrison, G.S. Settles, A.A. Zheltovodov, A.I. Maksimov and A.M. Shevchenko, and S. S. Vorontsov : Asymmetric Crossing-Shock-Wave/Turbulent-Boundary-Layer Interaction, AIAA Jounal, Vol. 33, No. 12, December 1995
5. P. E. Rodi and D. S. Dolling : Behavior of Pressure and Heat Transfer in Sharp Fin-Induce Turbulent Interaction", AIAA Jounal, Vol. 33, No. 11, November 1995